



Article

# Dityrosine Crosslinking of Collagen and Amyloid- $\beta$ Peptides Is Formed by Vitamin B<sub>12</sub> Deficiency-Generated Oxidative Stress in *Caenorhabditis elegans*

Kyohei Koseki<sup>1</sup>, Aoi Yamamoto<sup>2</sup>, Keisuke Tanimoto<sup>3</sup>, Naho Okamoto<sup>1</sup>, Fei Teng<sup>4</sup>, Tomohiro Bito<sup>1,2,3,\*</sup> , Yukinori Yabuta<sup>1,2,3</sup> , Tsuyoshi Kawano<sup>1,2,3</sup> and Fumio Watanabe<sup>1,2,3</sup>

<sup>1</sup> The United Graduate School of Agricultural Sciences, Tottori University, Tottori 680-8553, Japan; kyouhei.ganbalu@gmail.com (K.K.); mizonbon26@gmail.com (N.O.); yabuta@tottori-u.ac.jp (Y.Y.); kawano@tottori-u.ac.jp (T.K.); watanabe@tottori-u.ac.jp (F.W.)

<sup>2</sup> Department of Agricultural Science, Graduate School of Sustainability Science, Tottori University, Tottori 680-8553, Japan; m21j7037b@edu.tottori-u.ac.jp

<sup>3</sup> Department of Agricultural, Life and Environmental Sciences, Faculty of Agriculture, Tottori University, Tottori 680-8553, Japan; b18a5103b@edu.tottori-u.ac.jp

<sup>4</sup> Department of Food Quality and Safety, College of Food Science, Northeast Agricultural University, Harbin 150030, China; tengfei@neau.edu.cn

\* Correspondence: bito@tottori-u.ac.jp; Tel.: +81-857-31-5443



**Citation:** Koseki, K.; Yamamoto, A.; Tanimoto, K.; Okamoto, N.; Teng, F.; Bito, T.; Yabuta, Y.; Kawano, T.; Watanabe, F. Dityrosine Crosslinking of Collagen and Amyloid- $\beta$  Peptides Is Formed by Vitamin B<sub>12</sub> Deficiency-Generated Oxidative Stress in *Caenorhabditis elegans*. *Int. J. Mol. Sci.* **2021**, *22*, 12959. <https://doi.org/10.3390/ijms222312959>

Academic Editor: Maurizio Battino

Received: 25 October 2021

Accepted: 26 November 2021

Published: 30 November 2021

**Publisher's Note:** MDPI stays neutral with regard to jurisdictional claims in published maps and institutional affiliations.

**Abstract:** (1) Background: Vitamin B<sub>12</sub> deficiency in *Caenorhabditis elegans* results in severe oxidative stress and induces morphological abnormality in mutants due to disordered cuticle collagen biosynthesis. We clarified the underlying mechanism leading to such mutant worms due to vitamin B<sub>12</sub> deficiency. (2) Results: The deficient worms exhibited decreased collagen levels of up to approximately 59% compared with the control. Although vitamin B<sub>12</sub> deficiency did not affect the mRNA expression of prolyl 4-hydroxylase, which catalyzes the formation of 4-hydroxyproline involved in intercellular collagen biosynthesis, the level of ascorbic acid, a prolyl 4-hydroxylase coenzyme, was markedly decreased. Dityrosine crosslinking is involved in the extracellular maturation of worm collagen. The dityrosine level of collagen significantly increased in the deficient worms compared with the control. However, vitamin B<sub>12</sub> deficiency hardly affected the mRNA expression levels of *bli-3* and *mlt-7*, which are encoding crosslinking-related enzymes, suggesting that deficiency-induced oxidative stress leads to dityrosine crosslinking. Moreover, using GMC101 mutant worms that express the full-length human amyloid  $\beta$ , we found that vitamin B<sub>12</sub> deficiency did not affect the gene and protein expressions of amyloid  $\beta$  but increased the formation of dityrosine crosslinking in the amyloid  $\beta$  protein. (3) Conclusions: Vitamin B<sub>12</sub>-deficient wild-type worms showed motility dysfunction due to decreased collagen levels and the formation of highly tyrosine-crosslinked collagen, potentially reducing their flexibility. In GMC101 mutant worms, vitamin B<sub>12</sub> deficiency-induced oxidative stress triggers dityrosine-crosslinked amyloid  $\beta$  formation, which might promote its stabilization and toxic oligomerization.

**Keywords:** Alzheimer's disease; ascorbic acid; *Caenorhabditis elegans*; collagen; dityrosine crosslinking; oxidative stress; vitamin B<sub>12</sub> deficiency



**Copyright:** © 2021 by the authors. Licensee MDPI, Basel, Switzerland. This article is an open access article distributed under the terms and conditions of the Creative Commons Attribution (CC BY) license (<https://creativecommons.org/licenses/by/4.0/>).

## 1. Introduction

Vitamin B<sub>12</sub> (B<sub>12</sub>) functions as the two coenzymes 5'-deoxyadenosylcobalamin and methylcobalamin of methylmalonyl-CoA mutase (EC 5.4.99.2) [1] and methionine synthase (MS; EC 2.1.1.13) [2], respectively, in mammals. Individuals deficient in B<sub>12</sub> reportedly showed a significant increase of intracellular homocysteine (Hcy), a potent prooxidant [3], due to the reduced activity of MS, catalyzing methionine synthesis from Hcy and N<sup>5</sup>-methyltetrahydrofolate [4]. Severe B<sub>12</sub> deficiency leads to various symptoms, such as

megaloblastic anemia, infertility, and neuropathy [3]. However, the underlying disease mechanisms are not fully understood [5,6].

As its molecular and cellular processes are similar to those of humans, *Caenorhabditis elegans* has been widely used as a model organism for genetic and biochemical studies. Our preceding study of B<sub>12</sub> deficiency using *C. elegans* showed the occurrence of B<sub>12</sub>-deficient worms with specific morphological abnormalities, like the short and plump “dumpy” mutant phenotype induced by the disordered biosynthesis of cuticular collagen, the main extracellular matrix component of the worm cuticle [7]. Mammalian collagen biosynthesis is well known to involve various posttranslational modifications [8], such as proline hydroxylation of collagen polypeptide chains in the rough endoplasmic reticulum and lysine oxidation of collagen triple helices in the extracellular space, catalyzed by prolyl 4-hydroxylase (EC 1.14.11.2) [9] and lysyl oxidase (EC 1.14.11.4) [10], respectively. Lysyl oxidase-derived linkages are predominantly formed in mammals during the extracellular maturation of the collagen molecule. However, lysyl crosslinking is absent from the *C. elegans* cuticle collagen [11]: it is replaced by dityrosine crosslinking [12]. No evidence has indicated whether B<sub>12</sub> deficiency could affect the intracellular biosynthesis and subsequent extracellular maturation of the worm cuticle collagen.

In this study, we demonstrated that B<sub>12</sub> deficiency results in significantly decreased collagen levels due to decreased ascorbic acid, a prolyl 4-hydroxylase coenzyme, and increased dityrosine crosslinking formation, leading to motility dysfunction. Furthermore, to the best of our knowledge, this study is the first to report that the dityrosine crosslinking of collagen was induced by oxidative stress generated by B<sub>12</sub> deficiency. The reactive oxygen species that induce dityrosine crosslinking are reportedly formed in the amyloid- $\beta$  (A $\beta$ ) oligomers involved in Alzheimer’s disease (AD) pathogenesis [13]. Therefore, our finding could be applied to evaluate whether B<sub>12</sub> deficiency could promote AD development. Using GMC101 mutant worms producing A $\beta$  peptides in their muscle cells, we also discussed how B<sub>12</sub> deficiency could affect the dityrosine crosslinking level of the A $\beta$  peptide in inducing oligomerization and toxicity.

## 2. Results

### 2.1. Effect of B<sub>12</sub> Deficiency on Collagen Biosynthesis in *C. elegans*

Figure 1A shows how B<sub>12</sub> deficiency affected worm body collagen levels, calculated from the hydroxyproline content determined by the amino acid analysis of hydrolyzed worm body proteins. The worm collagen level significantly decreased during B<sub>12</sub> deficiency. The decreased collagen level (approximately  $8.1 \pm 0.7$  mg/g wet weight) was approximately 59% of that of control worms. B<sub>12</sub> supplementation of B<sub>12</sub>-deficient worms completely recovered the reduced collagen level to that of the control (approximately  $14.8 \pm 0.4$  mg/g wet weight).

To clarify the underlying mechanism of significantly reduced collagen levels during B<sub>12</sub> deficiency, the prolyl 4-hydroxylase  $\alpha$  (PHY-1 and PHY-2) and  $\beta$  (PDI) subunits’ mRNA expressions were determined. As shown in Figure 1B, B<sub>12</sub> deficiency did not affect the prolyl 4-hydroxylase  $\alpha$  (*dpy-18* and *phy-2*) and  $\beta$  (*pdi-2*) subunits’ mRNA expressions.

Prolyl 4-hydroxylase requires L-ascorbic acid (AsA) as a coenzyme. Therefore, the AsA level was determined in the homogenates of the control and B<sub>12</sub>-deficient worms (Figure 1C). B<sub>12</sub> deficiency significantly reduced the AsA level (approximately  $22.3 \pm 5.2$   $\mu$ g/g wet weight), reaching approximately 52% of that of the control worms. B<sub>12</sub> supplementation of B<sub>12</sub>-deficient worms showed that the reduced AsA levels were completely recovered to that of the control (approximately  $45.3 \pm 2.6$   $\mu$ g/g wet weight). These results indicated that the significantly decreased collagen biosynthesis in B<sub>12</sub>-deficient worms was mainly due to the reduced level of AsA as a coenzyme of prolyl 4-hydroxylase, as the mRNA expression levels of the enzyme subunits were completely unaffected by the B<sub>12</sub> deficiency.

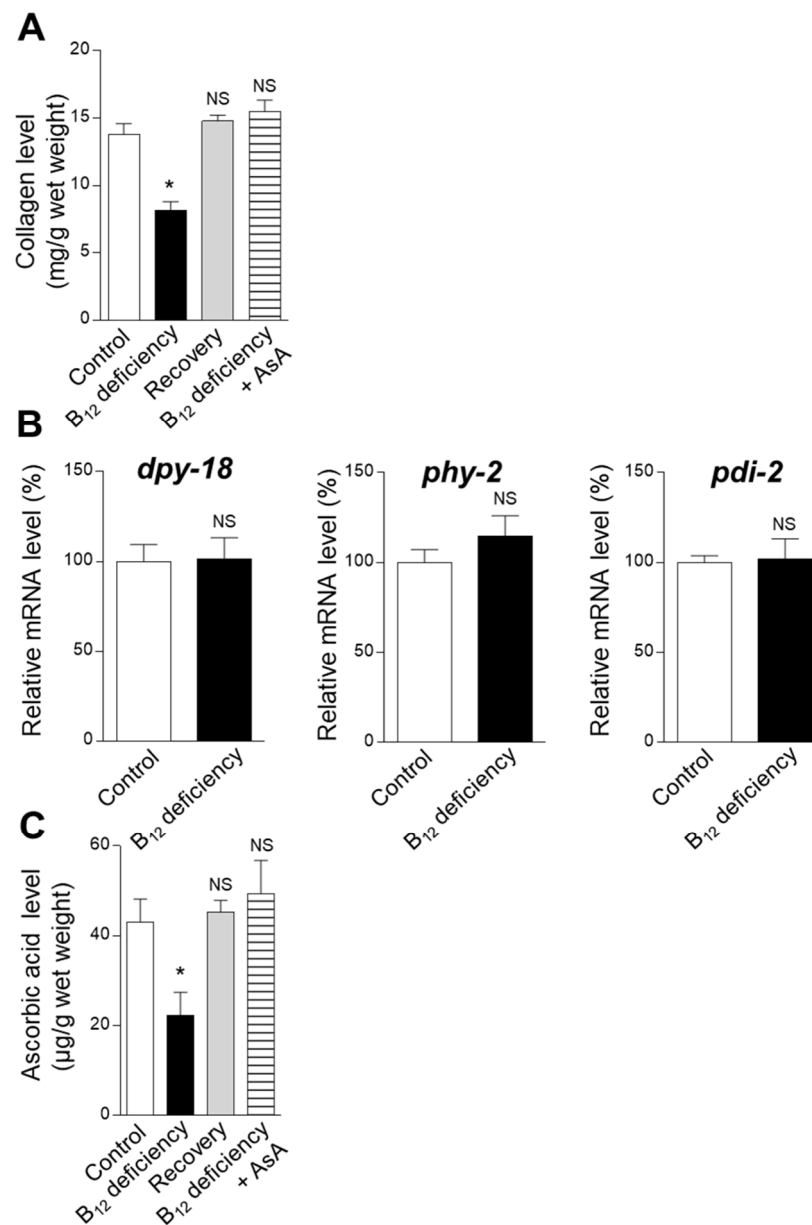


**Figure 1.** Effects of collagen biosynthesis during B<sub>12</sub> deficiency in *C. elegans*. (A) Collagen levels calculated from the hydroxyproline content, (B) the mRNA expression levels of genes encoding complex prolyl 4-hydroxylase proteins, and (C) vitamin C (AsA) levels determined in B<sub>12</sub>-supplemented worms (Control), B<sub>12</sub>-deficient worms (B<sub>12</sub> deficiency), B<sub>12</sub>-deficient worms grown for three generations under B<sub>12</sub>-supplemented conditions (Recovery), and B<sub>12</sub>-deficient worms grown for three generations under an AsA-supplemented condition (B<sub>12</sub> deficiency + AsA). Shown are the mRNA expression levels of human prolyl 4-hydroxylase subunit  $\alpha$ 1 (P4HA1) and prolyl 4-hydroxylase subunit  $\alpha$ 2 (P4HA2), and of prolyl 4-hydroxylase subunit  $\beta$  (P4HB) and their genetic orthologs *dpy-18*, *phy-2*, and *pdi-2*, respectively. The data represent the mean  $\pm$  SEM of three independent experiments (n = 3). \*  $p < 0.05$  versus the control group. NS represents no significant differences.

## 2.2. Effect of B<sub>12</sub> Deficiency on the Dityrosine Crosslinking Level of Worm Collagen

To clarify whether B<sub>12</sub> deficiency affects dityrosine crosslinking in the extracellular maturation of cuticular collagen, dityrosine levels were assayed in B<sub>12</sub>-deficient worms. Dityrosine levels (per mg collagen) significantly increased in the B<sub>12</sub>-deficient worms compared with control worms (Figure 2A). These results indicate that, although B<sub>12</sub> deficiency significantly reduces collagen levels, the dityrosine crosslinking level of collagen was

high. *bli-3* [14] and *mlt-7* [11] mRNA expression levels, encoding enzymes involved in the dityrosine crosslinking of worm collagen, were also tested. As shown in Figure 2B, B<sub>12</sub> deficiency hardly affected *bli-3* and *mlt-7* mRNA expression levels compared with those of the control. These results suggest that the dityrosine crosslinking of collagen is triggered by B<sub>12</sub> deficiency-induced oxidative stress.

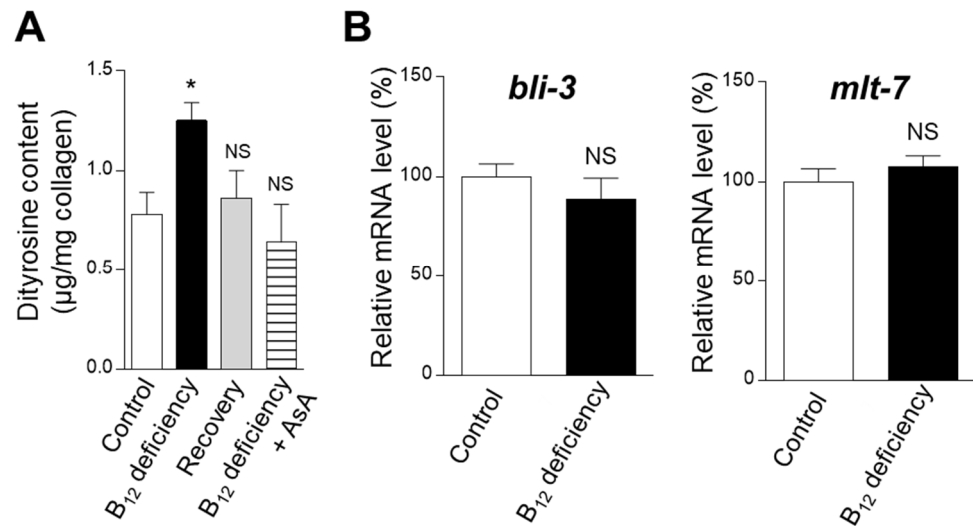


**Figure 2.** Effects of dityrosine and mRNA expression levels of enzymes involved in dityrosine crosslinking during B<sub>12</sub> deficiency in *C. elegans*. (A) Dityrosine (per 1 mg collagen) and (B) mRNA expression levels (*bli-3* and *mlt-7*) determined in B<sub>12</sub>-supplemented worms (Control), B<sub>12</sub>-deficient worms (B<sub>12</sub> deficiency), B<sub>12</sub>-deficient worms grown for three generations under B<sub>12</sub>-supplemented conditions (Recovery), and B<sub>12</sub>-deficient worms grown for three generations under AsA-supplemented conditions (B<sub>12</sub> deficiency + AsA). The data represent the mean ± SEM of three independent experiments (n = 3). \* *p* < 0.05 versus the control group. NS represents no significant differences.

### 2.3. Effect of Collagenase Treatment on the Cuticular Extracellular Matrix Epidermal Collagen Layer in Control and B<sub>12</sub>-Deficient Worms

To evaluate the effect of the highly formed dityrosine crosslinking of collagen, the epidermal collagen layer was treated with collagenase. When control and B<sub>12</sub>-deficient worms were treated with collagenase solution for 10 min, the epidermal collagen layer was mostly digested in the control worms but remained unaffected in the B<sub>12</sub>-deficient worms (Figure 3). When B<sub>12</sub>-deficient worms were grown for three generations under B<sub>12</sub>-supplemented conditions (recovery), the epidermal collagen layer of the recovery worms was readily digested by the collagenase treatment. These results indicate that the epidermal collagen layer of B<sub>12</sub>-deficient worms became collagenase-resistant due to the high-level dityrosine crosslinking, implying that cuticular collagen would become structurally stronger and more rigid in the B<sub>12</sub>-deficient worms compared with the control worms.

### 2.4. Effect of B<sub>12</sub> Deficiency on *C. elegans* Motility Function

The B<sub>12</sub> deficiency-induced high-level dityrosine crosslinking might potentially affect the physiological functions of the cuticular extracellular matrix. When the whiplash movement in the M9 buffer was evaluated as a motility function, the movement for 30 s in the B<sub>12</sub>-deficient worms (approximately 99.3 thrashes/30 s) was decreased up to approximately 80% of that of the control worms (approximately 125.9 thrashes/30 s) (Figure 4). The decreased motility function of B<sub>12</sub>-deficient worms was completely recovered to the control level when grown for three generations under B<sub>12</sub>-supplemented conditions (recovery). In addition, the AsA supplementation of B<sub>12</sub>-deficient worms showed that the reduced motility function was almost recovered to the control level. These results show that B<sub>12</sub> deficiency leads to worm motility dysfunction due to decreased collagen level and

increased dityrosine crosslinking formation in collagen, potentially reducing in flexibility of cuticular extracellular matrix.

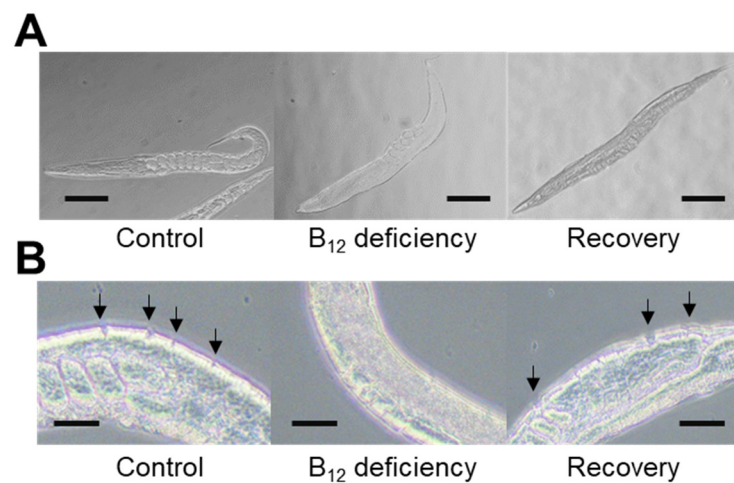


**Figure 3.** The morphological changes during B<sub>12</sub> deficiency and collagen layer states after collagenase treatment. **(A)** Each worm (approximately 100 individuals) was washed three times with M9 buffer (3 g KH<sub>2</sub>PO<sub>4</sub>, 6 g Na<sub>2</sub>HPO<sub>4</sub>, 0.5 g NaCl, and 1 g NH<sub>4</sub>Cl/L) and then imaged using a microscope system. Scale bars = 250 μm. **(B)** Each worm (approximately 100 individuals) was washed three times with the same M9 buffer and then fixed using 4% (*w/v*) paraformaldehyde for 10 min at 4 °C. The fixed worms were washed three times with PBS buffer (pH 7.2). Subsequently, the worms were soaked with 1.5 mL of β-mercaptoethanol buffer for 30 min using a rotator; then, the worms were washed three times with PBS buffer (pH 7.2). The washed worms were treated with collagenase solution for 10 min at room temperature and then kept on ice for 30 min to stop the reaction. Immediately after that, the worms were washed three times with PBS buffer (pH 7.2); then, each worm was mounted on glass slides. A microscope was used to observe the collagen layer. The arrow (↓) indicates the collagen layer decomposed by the collagenase treatment. Scale bars = 25 μm. Control, B<sub>12</sub> deficiency, and Recovery represent B<sub>12</sub>-supplemented worms, B<sub>12</sub>-deficient worms, and B<sub>12</sub>-deficient worms grown for three generations under B<sub>12</sub>-supplemented conditions, respectively.

### 2.5. Effect of B<sub>12</sub> Deficiency on the Dityrosine Crosslinking Level of Aβ Peptides in GMC101 Worms

Dityrosine crosslinks generated by reactive oxygen species are reportedly formed in Aβ oligomers, and these dityrosine links further stabilize the fibrils in developing AD [13]. To elucidate the relationship between B<sub>12</sub> deficiency and AD, we investigated whether reactive oxygen species induced by the B<sub>12</sub> deficiency significantly increased the dityrosine crosslinking levels of Aβ peptides using *C. elegans* GMC101 mutant worms producing Aβ<sub>1–42</sub> peptides in their muscle cells [15]. GMC101 mutant worms were grown until the young adult stage, under control and B<sub>12</sub>-deficient conditions; then, they were shifted from 20 °C to 25 °C to induce Aβ [15]. Half of the GMC101 worms grown under B<sub>12</sub>-deficient and control conditions showed signs of paralysis 48 and 96 h after the induction of Aβ, respectively (Figure 5). These results indicate that B<sub>12</sub> deficiency significantly promoted Aβ-induced paralysis in GMC101 mutant worms.

To evaluate how B<sub>12</sub> deficiency affects the Aβ mRNA and protein levels in GMC101 mutant worms, quantitative PCR and Western blot analyses were conducted. No significant changes could be observed between the control and B<sub>12</sub>-deficient mutant worm Aβ mRNA levels (Figure 6A). Figure 6B shows the protein expression levels in N2 wild-type and GMC101 mutant worms grown under B<sub>12</sub>-deficient and B<sub>12</sub>-supplemented conditions. Human Aβ antibody-immunoreactive components (A–F) were detected as oligomeric Aβ forms (approximately 17–31 kDa) only in GMC101 mutant worms, and monomeric Aβ (5 kDa) was not detected. An immunoreactive component with the molecular mass of 34 kDa was a non-specific component as the component was found in N2 wild-type

worms. As shown in Figure 6C, no significant difference in the immunoreactive component A–F could be detected between the B<sub>12</sub>-supplemented and B<sub>12</sub>-deficient GMC101 mutant worms.

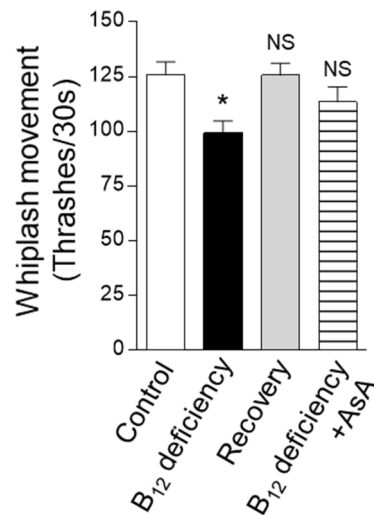


**Figure 4.** Effects of B<sub>12</sub> deficiency on *C. elegans* motility. Whiplash movement with underwater condition was determined in B<sub>12</sub>-supplemented (Control), B<sub>12</sub>-deficient (B<sub>12</sub> deficiency), B<sub>12</sub>-deficient worms grown for three generations under B<sub>12</sub>-supplemented conditions (Recovery), and B<sub>12</sub>-deficient worms grown for three generations under AsA-supplemented conditions (B<sub>12</sub> deficiency + AsA). The data represent the mean  $\pm$  SEM of whiplash movement of 50 individual animals. \*  $p < 0.05$  versus the control group. NS represents no significant differences.

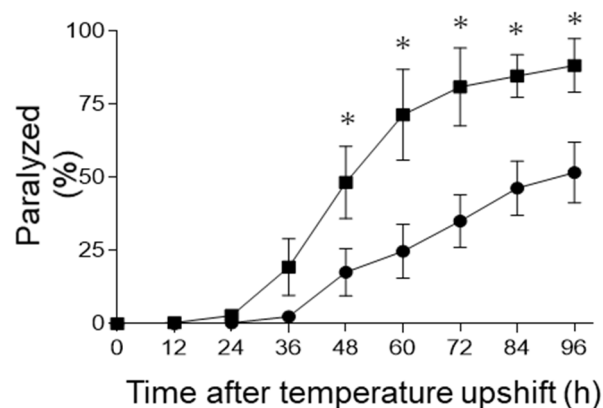


**Figure 5.** Paralysis rate of B<sub>12</sub>-supplemented and B<sub>12</sub>-deficient GMC101 mutants. When GMC101 mutants grown under B<sub>12</sub>-supplemented (●) and B<sub>12</sub>-deficient conditions (■) developed into young adults, each GMC101 strain was shifted from 20 °C to 25 °C for the A $\beta$  induction. The mean percentage of paralyzed worms is plotted against the time post temperature shift (h). All values represent the mean  $\pm$  SD of five independent experiments (N = 5). Approximately 250 worms were screened for each condition. Asterisks indicate significant differences compared with the B<sub>12</sub>-supplemented worms at the same time point (\*  $p < 0.05$ ).

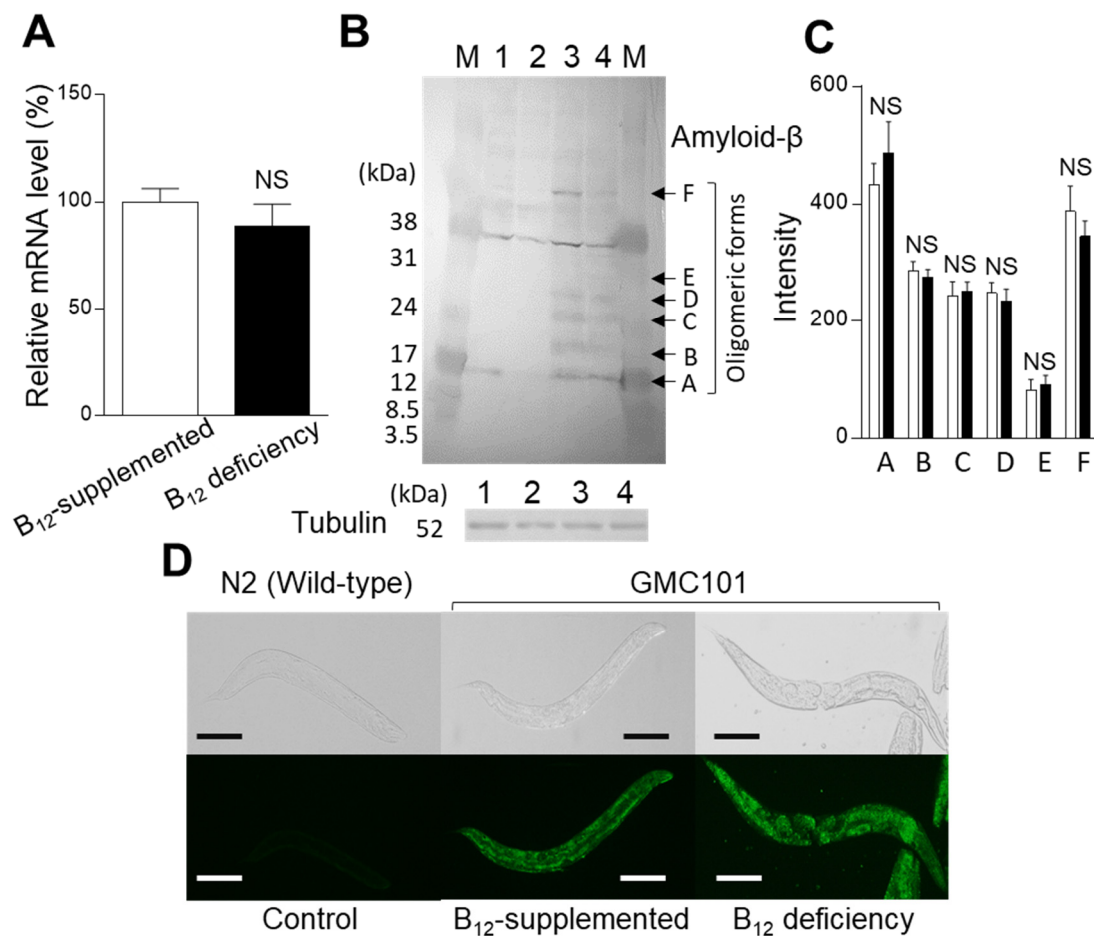


**Figure 6.** Effects of B<sub>12</sub> deficiency on the Aβ mRNA and protein expression levels in GMC101 mutants. **(A)** mRNA expression levels in B<sub>12</sub>-supplemented GMC101 mutant (B<sub>12</sub>-supplemented) and B<sub>12</sub>-deficient GMC101 mutant worms (B<sub>12</sub> deficiency). The data represent the mean ± SEM of three independent experiments. NS: no significant differences. **(B)** protein expression levels in B<sub>12</sub>-supplemented N2 wild-type worms (1), B<sub>12</sub>-deficient N2 wild-type worms (2), B<sub>12</sub>-supplemented GMC101 mutants (3), and B<sub>12</sub>-deficient GMC101 mutants (4). M: molecular mass marker proteins. A, B, C, D, E, and F: human Aβ anti-body-immunoreactive components (oligomeric Aβ forms). **(C)** Relative amounts of oligomeric Aβ forms in B<sub>12</sub>-supplemented (white bar) and B<sub>12</sub>-deficient (black bar) GMC101 mutants. Immunoreactive components A-F, detected in panel B, were quantified using the ImageJ software. The data represent the mean ± SEM of three independent experiments. NS: no significant differences. **(D)** Fluorescent images of Aβ in N2 wild-type and GMC101 mutant animals. B<sub>12</sub>-supplemented N2 (Control), B<sub>12</sub>-supplemented GMC101 mutants (B<sub>12</sub>-supplemented), and B<sub>12</sub>-deficient GMC101 mutants (B<sub>12</sub> deficiency). Scale bars = 200 μm.

However, B<sub>12</sub>-deficient GMC101 mutant worms appear to accumulate slightly more Aβ in the pharynx and tail compared with control mutant worms (Figure 6D), although quantitative differences cannot be shown. These results indicate that B<sub>12</sub> deficiency itself does not increase Aβ mRNA and protein expression levels.

To elucidate the effect of B<sub>12</sub> deficiency on the dityrosine crosslinking level of Aβ in GMC101 mutant worms, dityrosine crosslinking was investigated using a fluorescent microscope. The dityrosine crosslinking of Aβ was detected in the whole body of B<sub>12</sub>-deficient mutant, but not in control mutant worms (Figure 7). The significant dityrosine crosslinking found in B<sub>12</sub>-deficient mutant worms considerably decreased when grown for three generations under B<sub>12</sub>-supplemented conditions (Recovery). Moreover, the dityrosine crosslinking of Aβ could be hardly found in AsA-supplemented B<sub>12</sub>-deficient mutant worms.

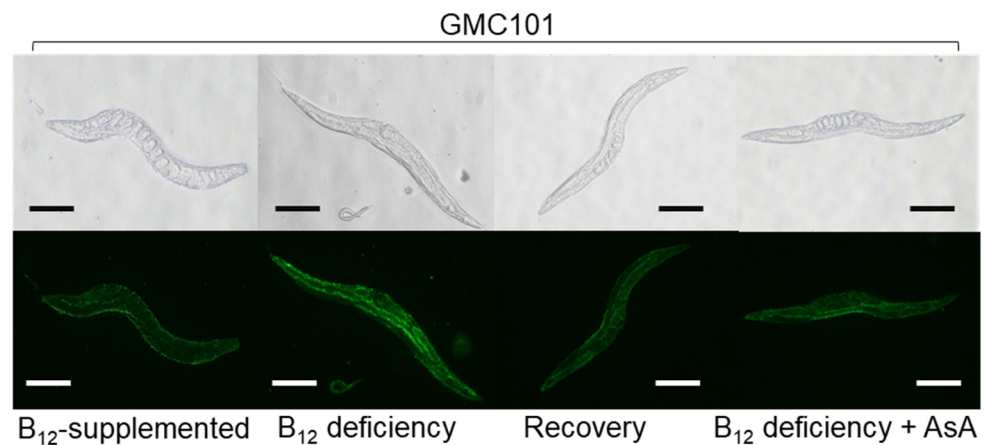


**Figure 7.** Dityrosine crosslinking accumulation in GMC101 mutants during B<sub>12</sub> deficiency. Fluorescent images of dityrosine in GMC101 mutants in B<sub>12</sub>-supplemented mutants (B<sub>12</sub>-supplemented), B<sub>12</sub>-deficient mutants (B<sub>12</sub> deficiency), B<sub>12</sub>-deficient mutants grown for three generations under B<sub>12</sub>-supplemented conditions (Recovery), and B<sub>12</sub>-deficient mutants grown in AsA-supplemented medium for three generations (B<sub>12</sub> deficiency + AsA). Scale bars = 200 μm.

To clarify whether B<sub>12</sub> deficiency-induced oxidative stress could promote the dityrosine crosslinking of Aβ, MDA and H<sub>2</sub>O<sub>2</sub> levels were determined in GMC101 mutant worms grown under control, B<sub>12</sub>-deficient, recovery, and AsA-supplemented B<sub>12</sub>-deficient conditions (Figure 8A,B). The MDA and H<sub>2</sub>O<sub>2</sub> levels significantly increased during B<sub>12</sub> deficiency. The increased MDA and H<sub>2</sub>O<sub>2</sub> levels of B<sub>12</sub>-deficient mutant worms were completely recovered to the control level when grown for three generations under B<sub>12</sub>-supplemented conditions (Recovery). Moreover, AsA supplementation did not show any increase in MDA and H<sub>2</sub>O<sub>2</sub> levels even in B<sub>12</sub>-deficient mutant worms. To evaluate the effects of B<sub>12</sub> deficiency on mRNA levels, encoding enzymes involved in cellular antioxidant systems, the superoxide dismutase (*sod-1*), and catalase (*ctl-1*) mRNA levels were measured by qPCR (Figure 8C). No significant changes in the *sod-1* and *ctl-1* mRNA levels were observed during B<sub>12</sub> deficiency. Although B<sub>12</sub> deficiency did not affect the mRNA levels of these antioxidant enzymes, it significantly increased the MDA and H<sub>2</sub>O<sub>2</sub> levels in GMC101 mutant worms, suggesting that superoxide dismutase and catalase activities decreased due to the oxidative inactivation of the enzymes, as described in B<sub>12</sub>-deficient N2 wild-type worms [16]. These observations indicate that B<sub>12</sub> deficiency-induced oxidative stress promoted the dityrosine crosslinking of Aβ.



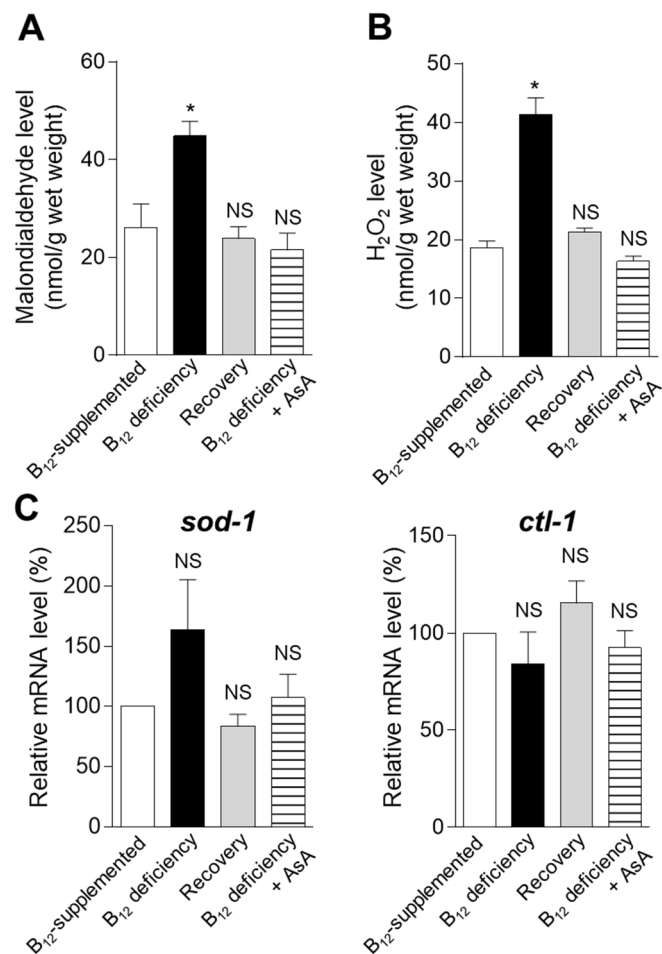


**Figure 8.** Effect of B<sub>12</sub> deficiency on oxidative stress marker and oxidative defense enzyme levels in GMC101 mutants. (A) MDA and (B) H<sub>2</sub>O<sub>2</sub> levels in GMC101 mutants are shown in B<sub>12</sub>-supplemented mutants (B<sub>12</sub>-supplemented), B<sub>12</sub>-deficient mutants (B<sub>12</sub> deficiency), B<sub>12</sub>-deficient mutants grown for three generations under B<sub>12</sub>-supplemented conditions (Recovery), and B<sub>12</sub>-deficient mutants grown in AsA-supplemented medium for three generations (B<sub>12</sub> deficiency + AsA). (C) Levels of mRNAs encoding enzymes involved in oxidant defense enzymes in GMC101 mutant animals. Using qPCR, we determined the levels of mRNAs encoding superoxide dismutase (*sod-1*) and catalase (*ctl-1*). The data represent the mean  $\pm$  SEM of three independent experiments. \*  $p < 0.05$  versus the control group. NS represents no significant differences.

### 3. Discussion

We previously reported that certain B<sub>12</sub>-deficient worms showed a short and plump phenotype, like “dumpy” mutants [7] formed due to the disordered cuticle collagen biosynthesis [17]. *C. elegans* possesses an external structure known as the cuticle, containing collagen and collagen-like protein major components of approximately 80% of the total cuticular protein content [18]. The cuticle is required to maintain body shape [19–21] and is synthesized five times from late embryogenesis throughout the *C. elegans* lifecycle, since the worm requires a new cuticle after molting in each growth stage [18]. Therefore, these observations indicate that the cuticle is crucial for the development and survival of worms. Worm cuticle collagen is synthesized and matured by the following steps. Synthesized collagen single polypeptides are modified with proline hydroxylation and disulfide bond formation by the proline hydroxylase complex [DPY-18 (*dpy-18*), PHY-2 (*phy-2*), and PDI (*pdi-2*)] in the rough endoplasmic reticulum. After the secretion of the modified collagen triple helices into the extracellular space, they undergo a final modification of an enzymatic intermolecular tyrosine crosslinking by a dual oxidase BLI-3 (*bli-3*) [11].

Although a *C. elegans* gene ortholog (*duox-2*) of the human dual oxidase 2, involved in collagen intermolecular crosslinking, has been identified [22], *duox-2* was not expressed in the worms [22,23], as this gene might be a pseudo-gene. Furthermore, a heme peroxidase MLT-7 (*mlt-7*), along with BLI-3, reportedly played an essential role in cuticle–collagen crosslinking [11]. In contrast, the occurrence of tyrosine crosslinking is rare in vertebrates, and lysyl oxidase-derived linkages are predominant, while lysyl crosslinking is absent in the *C. elegans* cuticle [11].

As shown in Figures 1B and 2B, B<sub>12</sub> deficiency did not affect the mRNA expression levels of the proline hydroxylase complex (DPY-18, PHY-2, and PDI), dual oxidase (BLI-3), and heme peroxidase (MLT-7) involved in the posttranslational modification of worm collagen. However, worm collagen level was significantly decreased to approximately 59% of that in the control during B<sub>12</sub> deficiency (Figure 1A). The decreased collagen level of B<sub>12</sub>-deficient worms was due to the significant decrease in AsA (approximately 52% of that of the control worms) (Figure 1C) as a coenzyme of prolyl 4-hydroxylase.

During B<sub>12</sub> deficiency, homocysteine (Hcy) was significantly accumulated in the worm body [7]; leading to the disruption of redox regulation [16] due to severe Hcy-related oxidative stress [24]. Although B<sub>12</sub> deficiency did not affect the mRNA expression levels of superoxide dismutase (*sod-1*) and catalase (*ctl-1*) involved in the cellular oxidant defense systems, the activities of superoxide dismutase and catalase were significantly reduced due to the oxidative inactivation of these enzymes [16]. Therefore, cellular antioxidant compound levels, such as those of glutathione and AsA were significantly reduced [16]. These observations indicate that AsA was mainly used as an antioxidant to scavenge oxidative stress induced during B<sub>12</sub> deficiency and, consequently, was significantly decreased. Therefore, the decreased AsA induced decreased collagen biosynthesis in *C. elegans*. AsA deficiency has reportedly interfered with collagen synthesis in guinea pigs [25]. Moreover, it has been reported that Hcy, itself, can disrupt the collagen posttranslational modification in mammalian bones [10,26,27].

As shown in Figure 2A, dityrosine levels (per mg collagen) were significantly increased in the B<sub>12</sub>-deficient worms compared with the control worms, indicating that B<sub>12</sub> deficiency significantly increases the crosslinking level of tyrosine residues in collagen. Tyrosine crosslinking was formed by reactive oxygen species, induced by significantly increased Hcy during B<sub>12</sub> deficiency, as B<sub>12</sub> deficiency hardly stimulated the mRNA expression levels of dual oxidase BLI-3 (*bli-3*) and the heme peroxidase MLT-7 (*mlt-7*) involved in the tyrosine crosslinking of the cuticular collagen. Lévine et al. [28] have reported that a deficiency of certain NADPH oxidase involved in the production of reactive oxygen species reduced dityrosine crosslinking, coinciding with the results of this study. Severe oxidative stress caused by aging has reportedly increased the dityrosine crosslinking of worm collagen [11].

The above-presented results suggest that the “dumpy” mutants formed by B<sub>12</sub> deficiency were due to reduced intracellular collagen biosynthesis. Furthermore, B<sub>12</sub> deficiency significantly increased the formation of the dityrosine crosslinking of collagen as an extracellular maturation step. As shown in Figure 4, B<sub>12</sub> deficiency leads to worm motility dysfunction, probably due to such disordered collagen biosynthesis and maturation, themselves being probably due to the reduction of cuticular extracellular matrix flexibility. Although thrashing rates generally reflect worm body wall muscles, we have no information available on whether B<sub>12</sub> deficiency-induced structural or functional muscular disorders.

Although little information is available on the mechanism by which B<sub>12</sub> deficiency contributes to AD pathogenesis, numerous studies have reported that the serum Hcy, elevated by B<sub>12</sub> deficiency, is associated with AD pathogenesis [29–31]. In this study, dityrosine crosslinking of the cuticular collagen was formed by B<sub>12</sub> deficiency-induced oxidative stress. Similarly, oxidative stress due to B<sub>12</sub> deficiency can induce the dityrosine crosslinking of A $\beta$  peptides in developing AD, as A $\beta$  oligomers are formed by the dityrosine crosslinking generated by reactive oxygen species [13]. In GMC101 mutant worms, the MDA and H<sub>2</sub>O<sub>2</sub> levels significantly increased during B<sub>12</sub> deficiency, although no significant changes could be observed in the mRNA levels of the superoxide dismutase

(*sod-1*) and catalase (*ctl-1*) involved in cellular oxidant defense systems. Similar results were reported in B<sub>12</sub>-deficient N2 wild-type worms exhibiting oxidative inactivation of superoxide dismutase and catalase, leading to the disruption of redox regulation [16]. Therefore, we evaluated whether oxidative stress generated by B<sub>12</sub> deficiency can form toxic A $\beta$  oligomers using a GMC101 mutant worm that expresses full-length human A $\beta$  peptide in the muscle cells. When A $\beta$  oligomerization is formed and its toxicity is induced, mutant worms have shown paralysis [15]. Therefore, the GMC101 mutant worm has been used as a model animal of AD [32]. Our previous study [33] indicated that B<sub>12</sub> deficiency did not stimulate the production of A $\beta$  peptides in GMC101 mutant worms, although B<sub>12</sub>-deficient worms exhibited paralysis faster and more severely than B<sub>12</sub>-sufficient worms (control) did. As shown in Figure 5, similar results were obtained in this study. Furthermore, AsA-supplemented B<sub>12</sub>-deficient worms rescued the paralysis phenotype. However, AsA supplementation did not affect A $\beta$  peptide aggregations, suggesting that oxidative stress caused by elevated Hcy levels is an important factor in toxicity.

As shown in Figure 7, the dityrosine crosslinking of A $\beta$  was present in the entire bodies of B<sub>12</sub>-deficient mutant worms, but not in those of control mutant worms. The dityrosine crosslinking of A $\beta$  could hardly be found in AsA-supplemented B<sub>12</sub>-deficient mutant worms. As shown in Figure 6, no significant changes could be observed in A $\beta$  oligomerization between the control and B<sub>12</sub>-deficient mutant worms. However, the B<sub>12</sub>-deficient worms exhibited paralysis due to toxicity faster than control worms did (Figure 5). Sitkiewicz et al. [34] demonstrated that tyrosine crosslinking shifts the equilibrium toward more compact oligomer types, leading to highly toxic fibrils. Maina et al. [35] suggest that dityrosine crosslinking, specifically, promotes the stabilization, but not the induction or facilitation, of A $\beta$  assembly, and A $\beta$  exerts high-level toxicity at a stage when self-assembly is high. These observations and the results presented in worms suggest that the dityrosine crosslinking formed during B<sub>12</sub> deficiency promotes the formation and stabilization of the compact A $\beta$  oligomers that facilitate self-assembly to induce high toxicity, probably in neuronal cells specifically located in the pharynx and tail (Figure 6D).

## 4. Materials and Methods

### 4.1. Organisms

The N2 Bristol wild-type *C. elegans* strain was maintained at 20 °C on nematode growth medium (NGM) plates using the *Escherichia coli* OP50 strain as a food source [36]. B<sub>12</sub>-supplemented (control) and B<sub>12</sub>-deficient worms were prepared as previously described [7]. B<sub>12</sub>-deficient worms were transferred to a B<sub>12</sub>-supplemented medium for three generations and used as the recovery worms. In the case of L-ascorbic acid (AsA)-supplemented experiments, B<sub>12</sub>-deficient worms were grown in a B<sub>12</sub>-deficient medium containing AsA 2-glucoside (final concentration of 1 mM) for three generations [16]. The transgenic GMC101 mutant worm strain was obtained from the Caenorhabditis Genetics Center (University of Minnesota, Minneapolis, MN, USA). The mutant worms were backcrossed five times before experimental use. When the mutant worms developed into young adults, their cultivation temperature was shifted from 20 °C to 25 °C to induce A $\beta$ . B<sub>12</sub> deficiency was also induced in the case of the GMC101 mutant worms through the above-described method. All nematodes were synchronized to obtain an identical developmental stage for experimental use.

### 4.2. Worm Body Collagen Determination

The acid hydrolysis of worm-body proteins was conducted according to the modified method of Roach and Gehrke [37]. Briefly, the worms (approximately 0.05 g wet weight of each background) were homogenized in 500  $\mu$ L of 6-M HCl using a hand homogenizer (AS ONE Corp., Osaka, Japan). The homogenates were transferred into glass reaction tubes and supplemented with 6-M HCl (500  $\mu$ L), and the pressure of the reaction tubes was reduced. After the homogenates were hydrolyzed under reduced pressure at 110 °C for 24 h, the resulting hydrolysates were centrifuged at 15,000 $\times$  g for 10 min at 4 °C. Each supernatant

(250  $\mu\text{L}$ ) was diluted with an equal volume of 0.25 mol/L lithium citrate buffer (pH 2.2) (Fujifilm Wako Pure Chemical, Osaka, Japan) and filtered using a Millex<sup>®</sup>-LH membrane filter (Merck Millipore, Darmstadt, Germany). Hydroxyproline was analyzed using a fully automated amino acid analyzer (JEOL JLC-500/V, Nihon Denshi Datem Corp. Ltd., Tokyo, Japan). The worm collagen content was calculated from the determined hydroxyproline values using a conversion factor of 8.33 [19].

#### 4.3. AsA Determination

The worms (approximately 0.05 g wet weight of each background) were homogenized in 300  $\mu\text{L}$  of 5% (*w/v*) metaphosphoric acid solution on ice using a hand homogenizer (AS ONE). After the homogenates were centrifuged at  $15,000\times g$  for 10 min at 4 °C, the supernatants were used as samples. AsA was assayed according to the 2,4-dinitrophenyl hydrazine derivatization method [38]. Briefly, after AsA was completely oxidized to dehydro-form using indophenol solution, the formed dehydroAsA was derivatized with 2,4-dinitrophenyl hydrazine to form its osazone. The formed derivative compound was determined using a Shimadzu High-Performance Liquid Chromatography (HPLC) system (SPD-6AV UV-VIS Spectrophotometric Detector, LP-6A Liquid Delivery Pump, and CTO-6V Column Oven) with a CDS ver. 5 chromat-data processing system (LASoft, Ltd., Chiba, Japan). Each sample (20  $\mu\text{L}$ ) was applied onto a Normal Phase HPLC Column (Senshu Pak Silica-2150-N,  $\phi$  6.0  $\times$  150 mm, Senshu Scientific Corp. Ltd., Tokyo, Japan) and eluted with acetic acid/hexane/ethyl acetate (1:4:5, *v/v/v*) as a mobile phase at 40 °C. The flow rate was 1.5 mL/min. The derivative compound was monitored by measuring the absorbance at 495 nm.

#### 4.4. Dityrosine Determination

Dityrosine was determined using the Shimadzu HPLC system (PU-2080 Plus Intelligent HPLC Pump, DG-2080-53 Degasser, RF-530 Fluorescence HPLC Monitor, and CTO-20A Column Oven) according to the method of Thein et al. [11]. Briefly, each hydrolyzed worm protein sample (20  $\mu\text{L}$ ), prepared as described above, was loaded onto a reversed-phase HPLC column (Luna C18 (2) 5  $\mu\text{m}$ , 250 mm  $\times$  4.6 mm 100 Å; Phenomenex, Torrance, CA, USA) and isocratically eluted with 0.1-M  $\text{KH}_2\text{PO}_4$ -phosphoric acid (pH 3.8) as a mobile phase, at 40 °C. The flow rate was 1 mL/min. Dityrosine was monitored by measuring the fluorescence with an excitation and emission at 285 and 410 nm, respectively.

#### 4.5. Collagenase Treatment

Worms (approximately 100 individuals) grown under various conditions were washed three times with M9 buffer (3 g  $\text{KH}_2\text{PO}_4$ , 6 g  $\text{Na}_2\text{HPO}_4$ , 0.5 g NaCl, and 1 g  $\text{NH}_4\text{Cl}$ /L) and then fixed with 4% (*w/v*) paraformaldehyde for 10 min at 4 °C. The fixed worms were washed three times with phosphate-buffered saline (PBS) buffer (pH 7.2). After the worms were soaked with 1.5 mL of  $\beta$ -mercaptoethanol buffer containing  $\beta$ -mercaptoethanol (75  $\mu\text{L}$ ), distilled water (1222.5  $\mu\text{L}$ ), 1 M Tris-HCl (pH 6.9) (187.5  $\mu\text{L}$ ), and Triton X-100 (15  $\mu\text{L}$ ) for 30 min using a rotator, they were washed three times with PBS buffer (pH 7.2). The washed worms were treated with 450  $\mu\text{L}$  of collagenase solution (1 unit/ $\mu\text{L}$ ) for 10 min at room temperature (25 °C), and the reaction vessel was placed on ice for 30 min to stop the enzyme reaction. After the treated worms were immediately washed three times with PBS buffer (pH 7.2), each worm was mounted on glass slides. The *C. elegans* cuticular collagen layer was observed under an ECLIPSE Ts2 microscope (Nikon Corp., Tokyo, Japan).

#### 4.6. Assays of Malondialdehyde and $\text{H}_2\text{O}_2$ as Oxidative Stress Markers

Worms (approximately 0.05 g wet weight of each background) grown under various conditions were homogenized in 200  $\mu\text{L}$  of 100 mM potassium-phosphate buffer (pH 7.0) on ice using a hand homogenizer (AS ONE). After the homogenates were centrifuged at  $15,000\times g$  for 10 min at 4 °C, the supernatants were used as samples. Malondialdehyde (MDA) and  $\text{H}_2\text{O}_2$  were determined using a TBARS assay kit (ZeptoMetrix Corp., Buffalo,

NY, USA) and a H<sub>2</sub>O<sub>2</sub> assay kit (BioVision, Inc., Milpitas, CA, USA), respectively. The MDA–thiobarbituric acid adducts or the reaction product of the OxiRed probe and H<sub>2</sub>O<sub>2</sub> in the presence of horseradish peroxidase formed in the samples were determined by measuring the absorbance at 540 or 570 nm, respectively, using a Sunrise Rainbow RC-R microplate reader (Tecan Austria GmbH, Salzburg, Austria).

#### 4.7. Immunofluorescent Staining of A $\beta$ and Dityrosine in GMC 101 Mutant Worms

For visualizing A $\beta$  peptides and their dityrosine crosslinking in the worm body, worms (approximately 100 individuals), grown under veracious conditions, were washed three times with M9 buffer and then fixed using 4% (*w/v*) paraformaldehyde for 10 min at 4 °C. The fixed worms were washed three times with PBS buffer (pH 7.2). After the worms were soaked with 1.5 mL of  $\beta$ -mercaptoethanol buffer, as described above, for 30 min using a rotator, they were washed three times with PBS buffer (pH 7.2). The washed worms were treated with 450  $\mu$ L of collagenase solution (1 unit/ $\mu$ L) for 13 or 15 min at room temperature (25 °C), and the reaction vessel was placed on ice for 30 min to stop the enzyme reaction. The treated worms were immediately washed three times with PBS buffer (pH 7.2) and then were treated with 500  $\mu$ L of blocking solution [5 mg bovine serum albumin (BSA) and 5  $\mu$ L Triton X-100 per 1 mL of PBS (pH 7.2)] for 30 min at room temperature (25 °C) to block nonspecific antibody binding. The treated worms were washed three times with a washing buffer [3 mg BSA and 5  $\mu$ L Triton X-100 per 1 mL of PBS (pH 7.2)]. After the worms were treated with an anti- $\beta$  amyloid 1-42 rabbit monoclonal antibody (ab180956, Abcam, Cambridge, MA, USA) or an anti-dityrosine mouse monoclonal antibody (Nikken Seil Co., Ltd., Shizuoka, Japan) for 24 h at room temperature (25 °C), they were washed with the abovementioned washing buffer. The worms were treated with an anti-rabbit IgG secondary antibody (20-fold dilution) (ab6717, Abcam) or an anti-mouse IgG secondary antibody (20-fold dilution) (ab6785, Abcam) coupled to fluorescein isothiocyanate under dark conditions for 1 h. Next, the worms were washed with the above-described washing buffer and mounted on glass slides. A $\beta$  and dityrosine visualization in the worms was performed using an ECLIPSE Ts2 fluorescent microscope (Nikon Corp.).

Immunoblot analysis was performed as previously described [33]. Sodium dodecyl sulfate polyacrylamide gel electrophoresis was performed using p-PAGEL slab gels (P-T16.5S; ATTO Corp., Tokyo, Japan). A $\beta$  peptide was detected using a monoclonal anti-A $\beta$ <sub>1-42</sub> primary antibody (EPR9296, Abcam) and anti-rabbit IgG-horseradish peroxidase conjugate (ab6721, Abcam). Signals were detected using EzWestBlue (ATTO Corp.) according to the manufacturer's instructions. The chemical coloring intensity was quantified using ImageJ (ImageJ Software, Bethesda, MD, USA) for three independent experiments.

#### 4.8. Quantitative Polymerase Chain Reaction (qPCR) Analysis

Worm total RNA was prepared using Sephasol<sup>®</sup>-RNA1 (Nacalai Tesque Inc., Kyoto, Japan). Poly(A)<sup>+</sup> mRNA was prepared from the total RNA using the Poly (A)<sup>+</sup> Isolation Kit from Total RNA (Nippon Gene, Tokyo, Japan) and then was used to synthesize cDNA using a PrimeScript<sup>™</sup> II 1st Strand cDNA Synthesis Kit (Takara Bio, Otsu, Japan). The primer pairs used for the qPCR analysis were designed using the GENETYX software (GENETYX Corp., Tokyo, Japan) to yield 20–24-nucleotide sequences with approximately 100–150-bp amplification products. A CFX Connect<sup>™</sup> Real-Time System (Bio-Rad) with SYBR Premix Ex Taq (Takara Bio) was used to perform qPCR.  $\beta$ -Actin (*act-1*) was used as an internal standard. The qPCR experiments were repeated at least three times for each cDNA prepared from three preparations of worms. Table 1 shows the primers used for qPCR.

**Table 1.** Primer pairs used for the qPCR analysis.

Genes	Sequence (5′–3′)
<i>dpy-18</i> (Sense)	CTACCACACTGTGATGTGGATG
<i>dpy-18</i> (Antisense)	GCGTGCTTCAAGTTGTTCTG
<i>phy-2</i> (Sense)	GCTTGATGTGTGGATGCAGGTT
<i>phy-2</i> (Antisense)	TTGCGAGTCGTTTGGTGAGA
<i>pdi-2</i> (Sense)	CGGAATCGATGATGTTCCATTCCG
<i>pdi-2</i> (Antisense)	TTGGGTGAGCTTCTCGTCGAAAG
<i>bli-3</i> (Sense)	GCGCTCAAAACATGTGCTGT
<i>bli-3</i> (Antisense)	GCCAGATTGTTGTACCATTCCGT
<i>mlt-7</i> (Sense)	TTGCGATCATCACGAGTGGTGT
<i>mlt-7</i> (Antisense)	AGCAGTTGTCGTGACTGGCAAA
A $\beta$ (Sense)	GCGGATGCAGAATCCGACATGAC
A $\beta$ (Antisense)	TATGACAACACCGCCCACCATGAG
<i>sod-1</i> (Sense)	TCTTCTCACTCAGGTCTCCAAC
<i>sod-1</i> (Antisense)	TCCGACTTCTGTGTGATCCA
<i>ctl-1</i> (Sense)	ATTATGCTCGTGGTGGAAACCC
<i>ctl-1</i> (Antisense)	ACAATGTTTGGCGCCCTCAA
<i>act-1</i> (Sense)	TCCAAGAGAGAGGTATCCTTACCC
<i>act-1</i> (Antisense)	CTCCATATCATCCCAGTTGGTG

The qPCR primer pairs were designed using the GENETYX software. For normalization,  $\beta$ -actin (*act-1*) served as the internal standard.

#### 4.9. Swim Locomotion Analysis

Worm motility function was evaluated using the swim locomotion method as follows. Individual three-day-old worms were placed on NGM agar plates (diameter of 3 cm) filled with 1.5 mL M9 buffer; then, their swimming motion was video-recorded for 1 min using a microscope (ECLIPSE Ts2, Nikon Corp.) equipped with a video system (DS-Fi3 camera unit and DS-L4 DS camera controller unit, Nikon Corp.). One round trip of worm head in the M9 buffer was determined as one whiplash movement.

#### 4.10. Paralysis Assay

GMC101 mutant worms were grown at 25 °C after the L4 stage for A $\beta$  induction. Worms that could move their heads but failed to move their bodies were scored as paralyzed [39]. The paralysis assay was performed every 12 h using approximately 50 individual worms.

#### 4.11. Statistical Analysis

The results shown in Figure 1A,C, Figures 2A, 4 and 8 were analyzed using one-way ANOVA with Bonferroni's post hoc test using GraphPad Prism 4 (GraphPad Software, La Jolla, CA, USA). The results shown in Figures 1B, 2B, 5 and 6A,C were analyzed using Student's *t*-test for pairwise comparison. All data, except for those presented in Figure 5, are presented as the mean  $\pm$  SEM. Differences were considered statistically significant at  $p < 0.05$ .

**Author Contributions:** Conceptualization, K.K., T.B. and F.W.; methodology, K.K., A.Y., K.T., N.O., F.T. and T.B.; software, K.K., N.O. and T.B.; validation, K.K., A.Y., K.T., N.O., F.T. and T.B.; formal analysis, K.K., A.Y., K.T., N.O., F.T. and T.B.; investigation, K.K., A.Y., K.T., N.O., F.T. and T.B.; resources, Y.Y. and T.K.; data curation, K.K., N.O. and T.B.; writing—original draft preparation, K.K., N.O., T.B. and F.W.; writing—review and editing, K.K., A.Y., K.T., N.O., T.B., Y.Y., T.K. and F.W.; visualization, K.K., A.Y., K.T. and T.B.; supervision, T.B. and F.W.; project administration, T.B. and F.W.; funding acquisition, T.B. and F.W. All authors have read and agreed to the published version of the manuscript.

**Funding:** This work was supported in part by JSPS KAKENHI Grant Numbers 19K15767 (T.B.) and 20580132 (F.W.).

**Institutional Review Board Statement:** Not applicable.

**Informed Consent Statement:** Not applicable.

**Data Availability Statement:** Data sharing not applicable.

**Conflicts of Interest:** The authors declare no conflict of interest.

## References

1. Sokolovskaya, O.M.; Plessl, T.; Bailey, H.; Mackinnon, S.; Baumgartner, M.R.; Yue, W.W.; Froese, D.S.; Taga, M.E. Naturally occurring cobalamin (B<sub>12</sub>) analogs can function as cofactor for human methylmalonyl-CoA mutase. *Biochimie* **2021**, *183*, 35–43. [CrossRef]
2. Froese, D.S.; Fowler, B.; Baumgartner, M.R. Vitamin B<sub>12</sub>, folate, and the methionine remethylation cycle—Biochemistry, pathways, and regulation. *J. Inherit. Metab. Dis.* **2018**, *42*, 673–685. [CrossRef]
3. Institute of Medicine (US) Standing Committee on the Scientific Evaluation of Dietary Reference Intakes and Its Panel on Folate, Other B Vitamins, and Choline. *Dietary Reference Intakes for Thiamin, Riboflavin, Niacin, Vitamin B6, Folate, Vitamin B12, Pantothenic Acid, Biotin, and Choline*; National Academies Press: Washington, DC, USA, 1998.
4. Lu, S.C. S-Adenosylmethionine. *Int. J. Biochem. Cell Biol.* **2000**, *32*, 391–395. [CrossRef]
5. Pepper, M.R.; Black, M.M. B<sub>12</sub> in fetal development. *Semin. Cell Dev. Biol.* **2011**, *22*, 619–623. [CrossRef]
6. Ebara, S.; Toyoshima, S.; Matsumura, T.; Adachi, S.; Takenaka, S.; Yamaji, R.; Watanabe, F.; Miyatake, K.; Inui, H.; Nakano, Y. Cobalamin deficiency results in severe metabolic disorder of serine and threonine in rats. *Biochim. Biophys. Acta* **2001**, *1568*, 111–117. [CrossRef]
7. Bito, T.; Matsunaga, Y.; Yabuta, Y.; Kawano, T.; Watanabe, F. Vitamin B<sub>12</sub> deficiency in *Caenorhabditis elegans* results in loss of fertility, extended life cycle, and reduced lifespan. *FEBS Open Bio* **2013**, *3*, 112–117. [CrossRef]
8. Kavitha, O.; Thampan, R.V. Factors influencing collagen biosynthesis. *J. Cell. Biochem.* **2008**, *104*, 1150–1160. [CrossRef]
9. Gorres, K.L.; Raines, R.T. Prolyl 4-hydroxylase. *Crit. Rev. Biochem. Mol. Biol.* **2010**, *45*, 106–124. [CrossRef]
10. Thaler, R.; Agsten, M.; Spitzer, S.; Paschalis, E.P.; Karlic, H.; Klaushofer, K.; Varga, F. Homocysteine suppresses the expression of the collagen cross-linker lysyl oxidase involving IL-6, Flil1, and Epigenetic DNA methylation. *J. Biol. Chem.* **2011**, *286*, 5578–5588. [CrossRef]
11. Thein, M.C.; Winter, A.D.; Stepek, G.; McCormack, G.; Stapleton, G.; Johnstone, I.L.; Page, A.P. Combined extracellular matrix cross-linking activity of the peroxidase MLT-7 and the dual oxidase BLI-3 is critical for post-embryonic viability in *Caenorhabditis elegans*. *J. Biol. Chem.* **2009**, *284*, 17549–17563. [CrossRef]
12. Ewald, C.Y. Redox signaling of NADPH oxidases regulates oxidative stress responses, immunity and aging. *Antioxidants* **2018**, *7*, 130. [CrossRef] [PubMed]
13. Al-Hilaly, Y.K.; Williams, T.L.; Stewart-Parker, M.; Ford, L.; Skaria, E.; Cole, M.; Bucher, W.G.; Morris, K.L.; Sada, A.A.; Thorpe, J.R.; et al. A central role for dityrosine crosslinking of amyloid- $\beta$  in Alzheimer's disease. *Acta Neuropathol. Commun.* **2013**, *1*, 83. [CrossRef] [PubMed]
14. Edens, W.A.; Sharling, L.; Cheng, G.; Shapira, R.; Kinkade, J.M.; Lee, T.; Edens, H.A.; Tang, X.; Sullards, C.; Flaherty, D.B.; et al. Tyrosine cross-linking of extracellular matrix is catalyzed by Duox, a multidomain oxidase/oxidoreductase with homology to the phagocyte oxidase subunit gp91phox. *J. Cell Biol.* **2001**, *154*, 879–892. [CrossRef] [PubMed]
15. Huang, J.; Chen, S.; Hu, L.; Niu, H.; Sun, Q.; Li, W.; Tan, G.; Li, J.; Jin, L.; Lyu, J.; et al. Mitoferrin-1 is involved in the progression of Alzheimer's disease through targeting mitochondrial iron metabolism in a *Caenorhabditis elegans* model of Alzheimer's disease. *Neuroscience* **2018**, *385*, 90–101. [CrossRef]
16. Bito, T.; Misaki, T.; Yabuta, Y.; Ishikawa, T.; Kawano, T.; Watanabe, F. Vitamin B<sub>12</sub> deficiency results in severe oxidative stress, leading to memory retention impairment in *Caenorhabditis elegans*. *Redox Biol.* **2017**, *11*, 21–29. [CrossRef]
17. Cai, L.; Phong, B.L.; Fisher, A.L.; Wang, Z. Regulation of fertility, survival, and cuticle collagen function by the *Caenorhabditis elegans* *eaf-1* and *ell-1* genes. *J. Biol. Chem.* **2011**, *286*, 35915–35921. [CrossRef]
18. Page, A.P.; Stepek, G.; Winter, A.D.; Pertab, D. Enzymology of the nematode cuticle: A potential drug target? *Int. J. Parasitol. Drugs Drug Resist.* **2014**, *4*, 133–141. [CrossRef]
19. Kramer, J.M. Structures and functions of collagens in *Caenorhabditis elegans*. *FASEB J.* **1994**, *8*, 329–336. [CrossRef]
20. Page, A.P.; Winter, A.D. Enzymes involved in the biogenesis of the nematode cuticle. *Adv. Parasitol.* **2003**, *53*, 85–148.
21. Wormbook. The Cuticle. Available online: <http://www.wormbook.org/index.html> (accessed on 2 October 2021).
22. Hill, A.A.; Hunter, C.P.; Tsung, B.T.; Tucker-Kellogg, G.; Brown, E.L. Genomic analysis of expression in *C. elegans*. *Science* **2000**, *290*, 809–812. [CrossRef]
23. Chávez, V.; Mohri-Shiomi, A.; Garsin, D.A. Ce-Duox1/BLI-3 generated reactive oxygen species as a protective innate immune mechanism in *Caenorhabditis elegans*. *Infect. Immun.* **2009**, *77*, 4983–4989. [CrossRef]
24. Škovierová, H.; Vidomanová, E.; Mahmood, S.; Sopková, J.; Drgová, A.; Červeňová, T.; Halašová, E.; Lehotský, J. The molecular and cellular effect of homocysteine metabolism imbalance on human health. *Int. J. Mol. Sci.* **2016**, *17*, 1733. [CrossRef]
25. Mahmoodian, F.; Peterkofsky, B. Vitamin C deficiency in guinea pigs differentially affects the expression of type 4 collagen, laminin, and elastin in blood vessels. *J. Nutr.* **1999**, *129*, 83–91. [CrossRef]
26. Clarke, M.; Ward, M.; Strain, J.J.; Hoey, L.; Dickey, W.; McNulty, H. B-vitamins and bone in health and disease: The current evidence. *Proc. Nutr. Soc.* **2014**, *73*, 330–339. [CrossRef] [PubMed]

27. Saito, M.; Marumo, K. The effects of homocysteine on the skeleton. *Curr. Osteoporos. Rep.* **2018**, *16*, 554–560. [[CrossRef](#)]
28. Lévigne, D.; Modarressi, A.; Krause, K.H.; Pittet-Cuénod, B. NADPH oxidase 4 deficiency leads to impaired wound repair and reduced dityrosine-crosslinking, but does not affect myofibroblast formation. *Free Radic. Biol. Med.* **2016**, *96*, 374–384. [[CrossRef](#)] [[PubMed](#)]
29. Chen, H.; Liu, S.; Ji, L.; Wu, T.; Ma, F.; Ji, Y.; Zhou, Y.; Zheng, M.; Zhang, M.; Huang, G. Associations between Alzheimer's disease and blood homocysteine, vitamin B<sub>12</sub>, and folate: A case-control study. *Curr. Alzheimer Res.* **2015**, *12*, 88–94. [[CrossRef](#)]
30. Liang, S.; Hong-Fang, J. Associations between homocysteine, folic acid, vitamin B<sub>12</sub> and Alzheimer's disease: Insights from meta-analyses. *J. Alzheimer's Dis.* **2015**, *46*, 777–790.
31. McLimans, K.E.; Martinez, A.D.C.; Mochel, J.P.; Allenspach, K. Serum vitamin B<sub>12</sub> and related 5-methyltetrahydrofolate-homocysteine methyltransferase reductase and cubilin genotypes predict neural outcomes across the Alzheimer's disease spectrum. *Br. J. Nutr.* **2020**, *124*, 135–145. [[CrossRef](#)]
32. Sorrentino, V.; Romani, M.; Mouchiroud, L.; Beck, J.S.; Zhang, H.; D'Amico, D.; Moullan, N.; Potenza, F.; Schmid, A.W.; Rietsch, S.; et al. Enhancing mitochondrial proteostasis reduces amyloid- $\beta$  proteotoxicity. *Nature* **2017**, *552*, 187–193. [[CrossRef](#)]
33. Andra, A.; Tanigawa, S.; Bito, T.; Ishihara, A.; Watanabe, F.; Yabuta, Y. Effects of vitamin B<sub>12</sub> deficiency on amyloid- toxicity in *Caenorhabditis elegans*. *Antioxidants* **2021**, *10*, 962. [[CrossRef](#)] [[PubMed](#)]
34. Sitkiewicz, E.; Oledzki, J.; Poznański, J.; Dadlez, M. Di-tyrosine cross-link decreases the collisional cross-section of A $\beta$  peptide dimers and trimers in the gas phase: An ion mobility study. *PLoS ONE* **2014**, *9*, e100200. [[CrossRef](#)] [[PubMed](#)]
35. Maina, M.B.; Mengham, K.; Burra, G.K.; Al-Hilaly, Y.A.; Serpell, L.C. Dityrosine cross-link trapping of amyloid- $\beta$  intermediates reveals that self-assembly is required for A $\beta$ -induced cytotoxicity. *bioRxiv* **2020**. [[CrossRef](#)]
36. Brenner, S. The genetics of *Caenorhabditis elegans*. *Genetics* **1974**, *77*, 71–94. [[CrossRef](#)] [[PubMed](#)]
37. Roach, D.; Gehrke, C.W. The hydrolysis of proteins. *J. Chromatogr. A* **1970**, *52*, 393–404. [[CrossRef](#)]
38. Standard Tables of Food Composition in Japan-2010. *The Council for Science and Technology, Ministry of Education, Culture, Sports, Science and Technology*; Official Gazette Co-Operation of Japan: Tokyo, Japan, 2010.
39. Gutierrez-Zepeda, A.; Santell, R.; Wu, Z.; Brown, M.; Wu, Y.; Khan, I.; Link, C.D.; Zhao, B.; Luo, Y. Soy isoflavone glycitein protects against beta amyloid-induced toxicity and oxidative stress in transgenic *Caenorhabditis elegans*. *BMC Neurosci.* **2005**, *6*, 54. [[CrossRef](#)]